

Conjugated Fluorene and Silole Copolymers: Synthesis, Characterization, Electronic Transition, Light Emission, Photovoltaic Cell, and Field Effect Hole Mobility

Feng Wang, Jie Luo, Kaixia Yang, Junwu Chen,* Fei Huang, and Yong Cao

Institute of Polymer Optoelectronic Materials & Devices, Key Laboratory of Specially Functional Materials and Advanced Manufacturing Technology of Ministry of Education, South China University of Technology, Guangzhou 510640, China

Received November 25, 2004; Revised Manuscript Received December 21, 2004

ABSTRACT: A novel series of soluble conjugated random and alternating copolymers (PFO-TST) derived from 9,9-dioctylfluorene (FO) and 1,1-dimethyl-3,4-diphenyl-2,5-bis(2'-thienyl)silole (TST) were synthesized by palladium(0)-catalyzed Suzuki coupling reactions. The feed ratios of FO to TST were 99:1, 95:5, 90:10, 80:20, and 50:50. Chemical structures and optoelectronic properties of the copolymers were characterized by elemental analysis, NMR, UV absorption, cyclic voltammetry, photoluminescence (PL), electroluminescence (EL), a photovoltaic cell, and a field effect transistor. The elemental analyses of the copolymers indicated that FO and TST contents in the copolymers were very close to the feed compositions. The random copolymers exhibited a PFO-segment-dominated UV absorption peak at ~ 385 nm and a narrow band gap TST absorption at ~ 490 nm. For the alternating copolymer, only a broad absorption band was found, demonstrating a mixed and TST-dominated electronic configuration. Compared with the solution PL, complete PL excitation energy transfer from the PFO segment to the TST unit could be achieved by film PL at lower TST content. It was found that the EL spectra of the copolymers with a device configuration of indium–tin oxide/poly(3,4-ethylenedioxythiophene)/poly(vinylcarbazole) (PVK)/copolymer/Ba/Al were red shifted and had better red light CIE coordinates with improved external quantum efficiency, compared with corresponding device performances without the PVK layer. With the alternating copolymer as the electron donor and methanofullerene [6,6]-phenyl C61-butyric acid methyl ester as the electron acceptor, an energy conversion efficiency of 2.01% was achieved under an AM1.5 simulated solar light at 100 mW/cm², which is among the highest values so far reported for bulk-heterojunction photovoltaic cells. The field effect hole mobility of the alternating copolymer is 4.5×10^{-5} cm²/(V s) using polyacrylonitrile as an organic insulator on a gate electrode.

Introduction

Conjugated polymers have drawn broad attention due to their important applications in polymeric light-emitting diodes (PLEDs),^{1,2} photovoltaic cells (PVCs),³ and field effect transistors (FETs).⁴ Ink-jet printing of PLEDs is the key advantages in the commercialization of full-color and large-area flat panel displays.⁵ Spin coating and the low cost of polymer-based PVCs are the attracting advantages for the fabrications of large-area solar cells.^{3d,6} Conjugated polymers are the best candidates to be used to fabricate flexible PLEDs, PVCs, and FETs. A notable feature of conjugated polymers also lies in the enormous versatility of the synthetic methodology, which affords wide space to construct new polymers with improved properties.

In the past decade, polyfluorenes (PFs) have emerged as emitting materials suitable for use in PLEDs because of their highly efficient photoluminescence (PL) and electroluminescence (EL), their thermal and oxidative stability, and their good solubility.⁷ Recently, amino-alkyl-substituted PFs or their quarternized salts were reported as novel electron injection layers for a high work function metal such as the Al cathode.⁸ Though PFs were typical blue-light-emitting polymers in the beginning due to the large band gap,⁹ thereafter green and red lights of PF copolymers were achieved by

incorporating narrow band gap comonomers into the PF backbone.^{10–12} Besides the color tuning for PLED applications, recently excellent PVC performances have also been achieved by some PF copolymers containing 2,1,3-benzothiadiazole derivatives.¹³

Siloles or silacyclopentadienes are a group of five-membered silacyclics that possess a unique low-lying LUMO level associated with the $\sigma^*-\pi^*$ conjugation arising from the interaction between the σ^* orbital of two exocyclic σ bonds on the silicon atom and the π^* orbital of the butadiene moiety.¹⁴ Siloles exhibit high electron acceptability^{14a} and fast electron mobility.¹⁵ 2,3,4,5-Tetraphenylsiloles show novel fluorescent characteristics (aggregation-induced emission).¹⁶ Excellent EL performances have been realized with 2,3,4,5-tetraphenylsiloles derivatives as the emissive layer.^{17,18} Recently, poly(di-*n*-hexylfluorene-co-4,4-diphenyldithienosilole) with low silole content ($\leq 10\%$) was reported by Jen and co-workers.¹⁹ Novel linear and hyperbranched 2,3,4,5-tetraphenylsilole-containing polymers were also demonstrated.²⁰ Siloles are narrow band gap building blocks for conjugated polymers.²¹ Thus, the incorporation of silole into the main chain of PF can probably afford copolymers with a new electron configuration and new optoelectronic properties. So far, there are few reports on silole-containing polymers as the emitting materials in EL devices, and they only exhibited blue and green emissions.^{19,20a} To the best of our knowledge, PVC and FET devices of silole-containing polymers were not reported before. In this work, a novel series of soluble conjugated random and alternating copolymers

* To whom correspondence should be addressed. E-mail: psjwchen@scut.edu.cn. Phone: +8620-8711-4346. Fax: +8620-8711-4535.

(PFO-TST) derived from 9,9-dioctylfluorene (FO) and 1,1-dimethyl-3,4-diphenyl-2,5-bis(2'-thienyl)silole (TST) were successfully synthesized by palladium(0)-catalyzed Suzuki coupling reactions. The optical and electronic properties such as UV absorption, electrochemical properties, photoluminescence, electroluminescence, photovoltaic cell properties, and field effect transistor properties of the copolymers were evaluated.

Experimental Section

Materials. All manipulations involving air-sensitive reagents were performed under an atmosphere of dry argon. All reagents, unless otherwise specified, were obtained from Aldrich, Acros, and TCI Chemical Co. and were used as received. All solvents were carefully dried and purified under nitrogen flow. Compounds 1,1-dimethyl-3,4-diphenyl-2,5-bis(2'-thienyl)silole (**1**),²² 2,7-bis(4,4,5,5-tetramethyl-1,3,2-dioxaborolan-2-yl)-9,9-dioctylfluorene (**3**),^{9b} and 2,7-dibromo-9,9-dioctylfluorene (**4**)^{9b} were prepared according to the literature, and all of them were recrystallized to reach the desirable purity for the next reactions.

Instrumentation. ¹H and ¹³C NMR spectra were recorded on a Bruker DRX 400 or AV 400 spectrometer with tetramethylsilane (TMS) as the internal reference. Molecular weights of the polymers were obtained on a Waters GPC 2410 using a calibration curve of polystyrene standards, with tetrahydrofuran as the eluent. Elemental analyses were performed on a Vario EL elemental analysis instrument (Elementar Co.). UV-vis absorption spectra were recorded on an HP 8453 spectrophotometer. The PL quantum yields were determined in an Integrating Sphere IS080 (LabSphere) with 405 nm excitation of a HeCd laser (Melles Griot). PL an EL spectra were recorded on an Instaspec IV CCD spectrophotometer (Oriol Co.). Cyclic voltammetry was carried out on a CHI660A electrochemical workstation with platinum electrodes at a scan rate of 50 mV/s against a saturated calomel reference electrode with a nitrogen-saturated solution of 0.1 M tetrabutylammonium hexafluorophosphate (Bu₄NPF₆) in acetonitrile (CH₃CN). The deposition of the copolymer on the electrode was done by the evaporation of a dilute chloroform solution.

1,1-Dimethyl-3,4-diphenyl-2,5-bis(5'-bromo-2'-thienyl)silole (2). *N*-Bromosuccinimide (NBS) (783 mg, 4.4 mmol) was dissolved in 20 mL of anhydrous DMF. This mixture was added dropwise to a mixture of **1** (853 mg, 2 mmol) in anhydrous DMF (25 mL) in the dark. The mixture was stirred for 15 min and poured into 100 mL of water. The organic material was extracted with dichloromethane (2 × 150 mL). The crude product was purified on a silica gel column using a petroleum ether/chloroform mixture (5:1 by volume) as eluent. A yellow solid of **2** was isolated in 45% yield (525 mg). Recrystallization from a toluene/heptane mixture gave 409 mg of pure compound. ¹H NMR (400 MHz, CDCl₃): δ (TMS, ppm) 7.16 (m, 6H, phenyl *H*), 6.93 (m, 4H, phenyl *H*), 6.80 (d, 2H, thienyl *H*), 6.64 (d, 2H, thienyl *H*), 0.63 (s, 6H, CH₃). ¹³C NMR (100 MHz, CDCl₃): δ (TMS, ppm) 152.9, 144.5, 138.3, 131.6, 129.3, 128.9, 128.7, 127.7, 127.0, 113.2, -1.9. GC-MS: *m/e* 584 (M⁺). Anal. Calcd for C₂₆H₂₀Br₂S₂Si: C, 53.42; H, 3.42; S, 10.96. Found: C, 53.37; H, 3.52; S, 10.78.

Polymerization. All of the polymerizations were carried out by palladium(0)-catalyzed Suzuki coupling reactions with an equivalent molar ratio of the diboronic ester monomer to the dibromo monomers under dry argon protection. The purifications of the polymers were conducted in air with yields of 68–80%. A typical procedure for the copolymerization is given below.

Carefully purified 2,7-bis(4,4,5,5-tetramethyl-1,3,2-dioxaborolan-2-yl)-9,9-dioctylfluorene (**3**) (642 mg, 1 mmol), 1,1-dimethyl-3,4-diphenyl-2,5-bis(5'-bromo-2'-thienyl)silole (**2**) (584 mg, 1 mmol), (PPh₃)₄Pd(0) (6 mg, 0.005 mmol), and several drops of Aliquat 336 were dissolved in a mixture of toluene (10 mL) and aqueous 2 M Na₂CO₃ (2 mL). The solution was refluxed with vigorous stirring for 48 h. At the end of the

Table 1. Molecular Weights and Elemental Analyses of the Copolymers

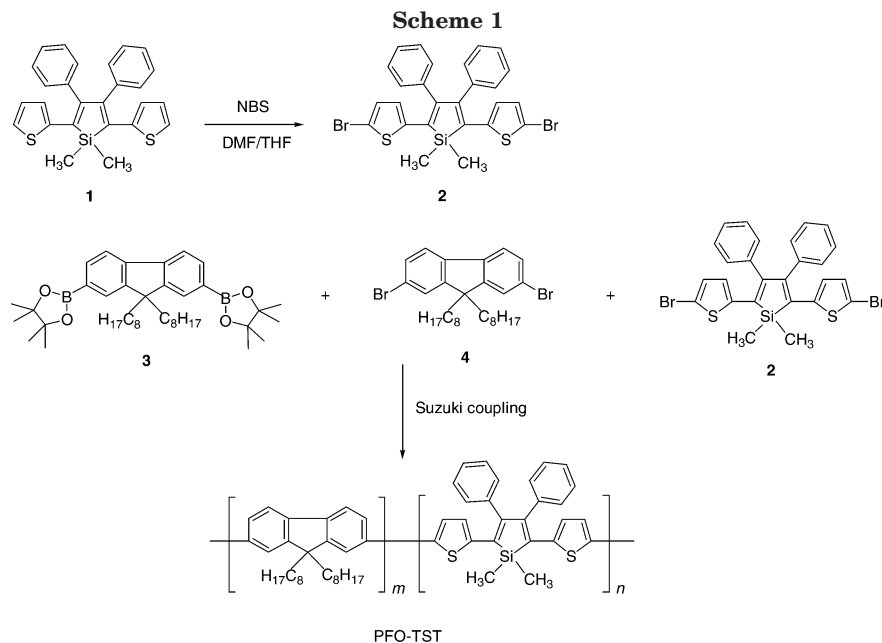
copolymer	<i>M_w</i> ^a	<i>M_w/M_n</i> ^a	elemental analysis ^b		
			C	H	S
PFO-TST1	29800	2.0	88.06 (89.62)	10.04 (10.36)	
PFO-TST5	35500	1.7	87.58 (88.75)	9.74 (10.07)	0.42 (0.82)
PFO-TST10	34700	1.9	86.74 (87.89)	9.50 (9.77)	1.56 (1.63)
PFO-TST20	32900	1.8	82.63 (86.17)	8.87 (9.17)	3.10 (3.24)
PFO-TST50	44400	1.4	80.28 (81.22)	7.58 (7.44)	7.49 (7.89)

^a Estimated by GPC in THF on the basis of a polystyrene calibration. ^b Data given in the parentheses are contents in the feed compositions.

polymerization, a small amount of **3** was added to remove the bromine end groups, and bromobenzene was added as a monofunctional end-capping reagent to remove the boronic ester end group because boron and bromine units could quench emission and contribute to excimer formation in LED application. The mixture was then poured into vigorously stirred methanol. The precipitated solid was filtered and washed for 24 h with acetone to remove oligomers and catalyst residues. A red powder of PFO-TST50 was isolated in 75% yield (610 mg). *M_w* = 44400, *M_w/M_n* = 1.4 (GPC, Table 1). ¹H NMR (400 MHz, CDCl₃): δ (TMS, ppm) 7.66–6.84 (m, br, 20H, Ar *H*), 1.91 (s, br, 4H, Ar CH₂), 1.27–1.03 (m, br, 20H, CH₂), 0.82 (m, br, 10H, CH₂ and CCH₃), 0.61 (s, br, 6H, SiCH₃). ¹³C NMR (100 MHz, CDCl₃): δ (TMS, ppm) 152.9, 151.5, 144.4, 142.5, 140.0, 139.1, 133.3, 131.9, 129.6, 128.6, 128.1, 127.2, 124.7, 122.4, 119.9, 119.6, 55.0, 40.3, 31.8, 30.0, 29.7, 29.2, 23.7, 22.6, 14.1, -1.7. Anal. Found: C, 80.28; H, 7.58; S, 7.49. UV (CHCl₃): λ_{max}/ε_{max} (mol⁻¹ L cm⁻¹) 510 nm/9.3 × 10³.

LED Fabrication and Characterization. Polymers were dissolved in toluene or *p*-xylene and filtered through a 0.45 μm filter. Patterned indium-tin oxide (ITO; ~15 Ω/square)-coated glass substrates were cleaned with acetone, detergent, distilled water, and 2-propanol, subsequently in an ultrasonic bath. After treatment with oxygen plasma, 150 nm of poly(3,4-ethylenedioxythiophene) doped with poly(styrenesulfonic acid) (PEDOT:PSS) (Baytron P 4083, Bayer AG) was spin-coated onto the ITO substrate followed by drying in a vacuum oven at 80 °C for 8 h. For some devices, poly(vinylcarbazole) (PVK; Aldrich) from 1,1,2,2-tetrachloroethane solution was coated on top of a dried PEDOT:PSS layer subsequently. A thin film of electroluminescent copolymer was coated onto the anode by spin-casting inside a nitrogen-filled drybox (Vacuum Atmospheres). The film thickness of the active layers was around 80 nm, as measured with an Alfa Step 500 surface profiler (Tencor). We note that since PVK is not soluble in *p*-xylene, PVK remains untouched during spinning of the top copolymer layer. A thin layer of Ba (4–5 nm) and subsequently 200 nm layers of Al were evaporated subsequently on the top of an EL polymer layer under a vacuum of 1 × 10⁻⁴ Pa. Device performances were measured inside a drybox (Vacuum Atmospheres). Current-voltage (*I*-*V*) characteristics were recorded with a Keithley 236 source meter. The luminance of the device was measured with a calibrated photodiode. The external quantum efficiency was verified by measurement in the integrating sphere (IS-080, Labsphere), and luminance was calibrated by using a PR-705 SpectraScan spectrophotometer (Photo Research) after encapsulation of the devices with UV-curing epoxy and a thin cover glass.

PVC Fabrication and Characterization. The PVC device structure used in this study was a sandwich structure, ITO/PEDOT:PSS/active layer/Ba/Al. ITO/PEDOT:PSS is the hole-collecting electrode, and Ba/Al is the electron-collecting electrode. We fabricated the PVC devices according to procedures similar to that of EL devices. The *I*-*V* characteristics in the dark and under illumination were measured with a Keithley 236 source meter. The photocurrent was measured under a solar simulator with AM1.5 illumination (100 mW/cm²). The spectral response was measured with a commercial photo-modulation spectroscopic setup including a xenon lamp, an optical chopper, a monochromator, and a lock-in amplifier



operated by a PC computer (Merlin, Oriol). A calibrated Si photodiode was used as a standard in the determination of photosensitivity.

FET Fabrication and Characterization. The configuration of the FET device is ITO/polyacrylonitrile (PAN)/PFO-TST50/Au. ITO on glass, used as the gate electrode, was patterned by photolithography. The thickness of the ITO measured by the surface profiler (Tencor, ALFA-Step 500) was 110 nm. PAN, the insulator for the gate electrode, was dissolved in *N,N*-dimethylformamide (DMF) and was deposited on top of the ITO by spin-coating. Then the PAN layer was dried at 90 °C for 20 h under vacuum, with a final thickness of 450 nm. To analyze the dielectric properties, we made a parallel capacitor with an ITO/insulator/Al structure. The capacitance was measured by a Hewlett-Packard 4192 impedance analyzer from 10 kHz to 1 MHz. On top of the dielectric layer, the active layer (PFO-TST50) was obtained by spinning of its toluene solution in a nitrogen atmosphere followed by an annealing step at a temperature of 70 °C for 1 h under a nitrogen atmosphere. The thickness of the active layer was 80 nm. On the top of the active layer, a gold layer with a thickness of 50 nm was thermally deposited in a vacuum through a shadow mask to obtain the source and drain electrodes. Thus, the channel was formed with an interdigital structure. The channel width-to-length ratio (*W/L*) was 100. The output characteristics were measured under a nitrogen atmosphere by a Keithley 2400 and a computer-controlled source meter (Keithley 236 source-measure units) that controlled the gate voltage and drain voltage, respectively. The drain current was also recorded by the Keithley 236 source-measure units.

Results and Discussion

Synthesis and Characterization. The general synthetic routes toward the monomers and polymers are shown in Scheme 1. We synthesized compound **1** according to identical procedures reported by Yamaguchi et al.²² Then monomer **2** was prepared in good yield by the bromination of **1** with NBS in the dark. Monomers **3** and **4** were prepared according to published procedures.^{9b} Monomers **2–4** were recrystallized to reach the desirable purity for copolymerization.

Conjugated copolymers derived from monomers **2–4** were prepared by palladium(0)-catalyzed Suzuki coupling reactions with an equivalent molar ratio of the diboronic ester monomer to the dibromo monomers. The monomer ratios of fluorene to silole are 99:1, 95:5, 90:

10, 80:20, and 50:50, and the corresponding copolymers are named PFO-TST1–50.²³ PFO-TST50 is an alternating copolymer, and PFO-TST1–20 are random copolymers. All the copolymers are soluble in common solvents such as chloroform, toluene, tetrahydrofuran, etc. The molecular weights of the copolymers are listed in Table 1. The M_w values of the copolymers are around $(3–4) \times 10^4$ with a polydispersity index (M_w/M_n) from 1.4 to 2.0. The alternating copolymer PFO-TST50 has the highest M_w and the narrowest molecular weight distribution. The elemental analyses of the copolymers are also listed in Table 1. The contents of C, H, and S of the copolymers are very close to the feed compositions, and the relatively larger deviation of the S content of PFO-TST5 may be attributed to the inherently low S content of the copolymer, which causes larger experimental error. Since S is derived from TST, the result demonstrated that the narrow band gap TST was incorporated in the copolymers nearly according to the feed ratios.

Figure 1 shows evolution of ^1H NMR spectra of the copolymers from low TST content to high TST content. The ^{13}C NMR spectrum of the alternating copolymer is shown in Figure 2. The spectrum indicates that the chemical structure of each monomer unit in the alternating copolymer is symmetric. We can assign some characteristic carbon resonance, including one carbon resonating at $\delta = -1.7$ ppm for SiCH_3 of TST, one carbon resonating at $\delta = 152.8$ ppm for the “ene” carbon at the 3- or 4-position of the silole ring,²⁴ one carbon at $\delta = 151.5$ ppm for the 10- or 13-position carbon of fluorene,^{9b} one carbon at $\delta = 55.0$ ppm for the 9-position carbon of fluorene, and the eight carbons resonating between 40.3 and 14.1 ppm for the *n*-octyl group of the fluorene. The NMR results confirm the chemical structure of the alternating copolymer (see the Experimental Section for details).

UV Absorption and Electrochemical Properties. The UV–vis absorption spectra of the copolymers in chloroform solutions are shown in Figure 3A. The random copolymers PFO-TST1–20 show absorption maxima of around 385 nm, which are from the fluorene segment. The absorption spectrum of PFO-TST1 is practically identical to that of the PFO homopolymer due to the very low content of TST. The absorption

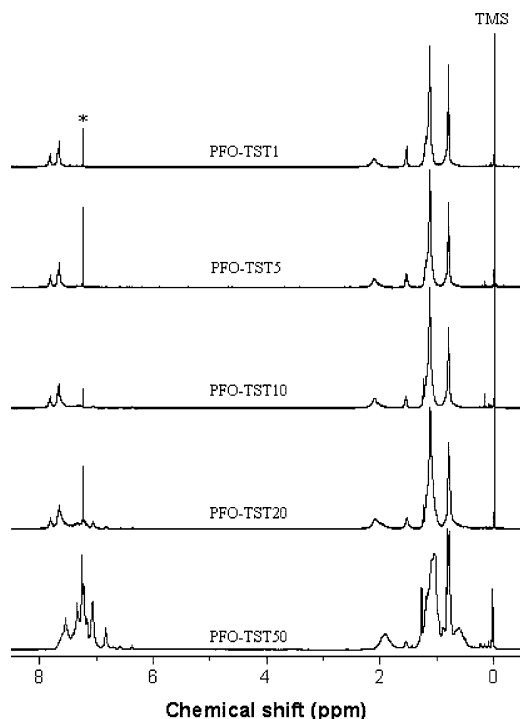


Figure 1. Evolution of ^1H NMR spectra of the copolymers from low TST content to high TST content (solvent CDCl_3). The solvent peaks are marked with an asterisk.

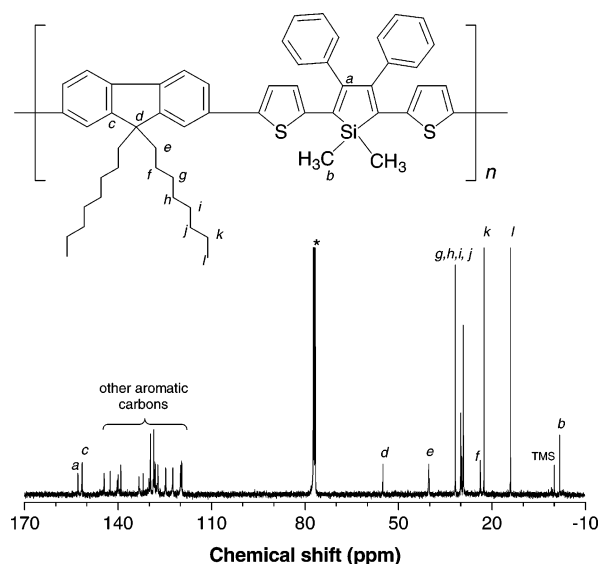


Figure 2. ^{13}C NMR spectrum of the alternating copolymer (PFO-TST50) in CDCl_3 . The solvent peaks are marked with an asterisk.

spectra of copolymers PFO-TST5–20 also show obvious absorptions at longer wavelengths, which are from the TST moiety. The higher the TST content in the random copolymer, the larger the absorbance ratio of TST to fluorene. The maxima of the TST absorption of PFO-TST5–20 are at 488, 488, and 495 nm, respectively. The alternating copolymer PFO-TST50 has a completely different absorption spectrum, compared with the random copolymers. The absorption peak at around 385 nm corresponding to the fluorene segment disappeared completely, and only a broad and strong absorption peaked at 510 nm, quite different from two separate absorptions of other alternating copolymers derived from fluorene and narrow band gap nitrogen-containing aromatic heterocyclics.^{12d,13a} The absorption spectrum

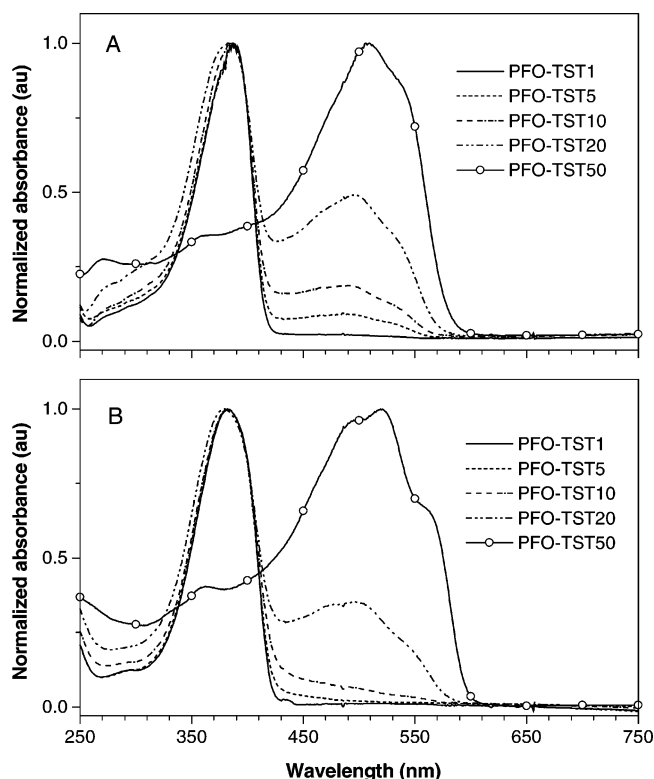


Figure 3. UV absorption spectra of the copolymers: (A) chloroform solution (1×10^{-4} M), (B) thin solid film.

Table 2. Optical Band Gaps and Electrochemical Properties of the Films of Copolymers

copolymer	optical band gap ^a (eV)	E_{ox} (V)	E_{red} (V)	HOMO ^c (eV)	LUMO ^d (eV)
PFO-TST1	2.95	1.35	-2.28	-5.75	-2.12
PFO-TST5	2.21 ^b	1.34	-2.29	-5.74	-2.11
PFO-TST10	2.15	1.35	-2.31	-5.75	-2.09
PFO-TST20	2.14	1.35	-0.80	-5.75	-3.60
PFO-TST50	2.08	1.31	-0.80	-5.71	-3.60

^a Estimated from the onset wavelength of optical absorption of the thin solid film. ^b Using the absorption spectrum of its chloroform solution. ^c Calculated according to $\text{HOMO} = -e(E_{\text{ox}} + 4.4)$. ^d Calculated according to $\text{LUMO} = -e(E_{\text{red}} + 4.4)$.

indicates that the electronic configurations of both components, fluorene and silole, in the alternating copolymer are mixed and silole-dominant.

The UV–vis absorption spectra of thin solid films of the copolymers are shown in Figure 3B. The absorption features of the films of the copolymers are similar to those of their chloroform solutions, but the TST absorption peaks of PFO-TST5 and PFO-TST10 are not so well-resolved, compared with those of the corresponding chloroform solutions. The TST absorption peak of the PFO-TST20 film is at 496 nm, which is practically identical to that of its chloroform solution. The TST absorption peak of the PFO-TST50 film is at 520 nm, with a 10 nm red shift to that of its chloroform solution. The optical band gaps of the films of the copolymers are estimated from the onset wavelengths of optical absorptions of thin solid films and are listed in Table 2. The optical band gap decreases with increasing TST content.

The electrochemical behavior of the copolymers was investigated by cyclic voltammetry (CV). We could record only one p-doping and one n-doping process of the copolymers. The onsets of oxidation processes of the copolymers are between 1.31 and 1.35 V (see Table 2), which are very close to the data reported for polyfluorene.

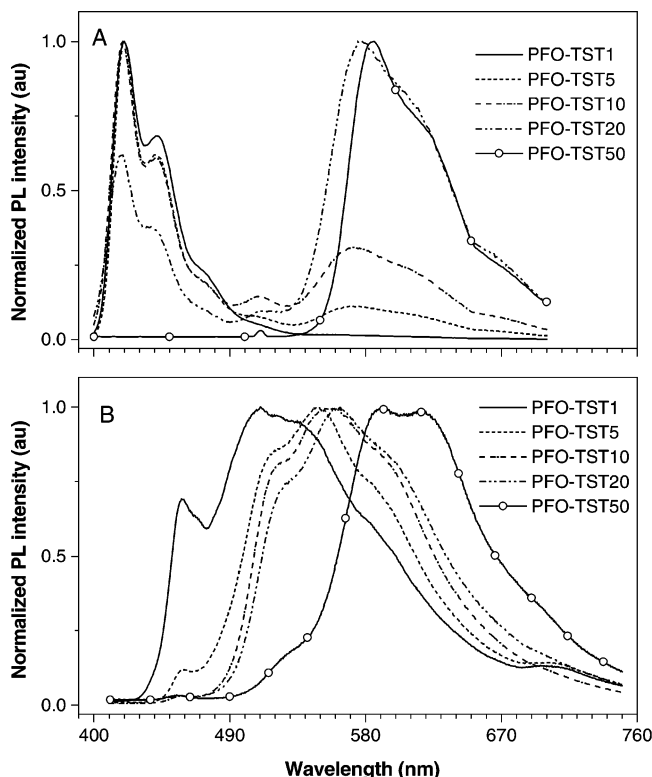


Figure 4. Photoluminescence spectra of the copolymers (excitation wavelength 390 nm): (A) chloroform solution (1×10^{-4} M), (B) thin solid film.

rene homopolymer, $E_{\text{ox}} = 1.4$ V and $I_p = 5.8$ eV.²⁵ So the oxidations are attributed to p-doping of PFO segments. The onsets of the n-doping processes of PFO-TST1–10 are between -2.28 and -2.31 V, which are the reductions of the PFO segments. The onsets of the n-doping processes of PFO-TST20 and PFO-TST50 are both at -0.80 V, which are the reductions of the TST moieties. The TST reduction was not found for PFO-TST1–10, probably due to the low TST contents in the copolymers. HOMO and LUMO levels calculated according to an empirical formula ($\text{HOMO} = -e(E_{\text{ox}} + 4.4)$ eV and $\text{LUMO} = -e(E_{\text{red}} + 4.4)$ eV)²⁶ are also listed in Table 2. The LUMOs of PFO-TST20 and PFO-TST50 demonstrate the low-lying LUMO structural characteristics of siloles. The electrochemical band gaps of PFO-TST1, PFO-TST20, and PFO-TST50 are very close to the corresponding optical band gap. The large deviations of the electrochemical band gap from the optical band gap of PFO-TST5 and PFO-TST10 indicate that the LUMOs of the two copolymers may not be reliable.

Photoluminescence Properties. Photoluminescence spectra of the copolymers in chloroform solution at a concentration of 1×10^{-4} M are shown in Figure 4A. The PL peaks are listed in Table 3. The feature of the PL spectrum of PFO-TST1 is completely PFO-dominant with two peaks at 418 and 441 nm. There is no signature of silole emission. Increasing the TST contents to 5%, the silole emission emerges with a maximum at 571 nm. The silole emission of PFO-TST10 is further enhanced but is still weaker than the PFO emission. The intensity of the silole emission of PFO-TST20 is stronger than that of the PFO emission, indicating the intramolecular energy transfer from the PFO segment to the silole moiety. For the alternating copolymer, there is only one peak at 585 nm, and the PFO emission disappears, demonstrating the important

Table 3. PL Properties of the Copolymers^a

copolymer	solution		QE ^b (%)
	λ_{max} (nm)	λ_{max} (nm)	
PFO-TST1	418, 441	458, 510	15.2
PFO-TST5	418, 441, 571	458, 549	24.8
PFO-TST10	418, 441, 572	557	20.0
PFO-TST20	418, 439, 577	562	12.1
PFO-TST50	585	591, 616	6.4

^a Excitation wavelength 390 nm. ^b Absolute PL quantum yield measured in the integrating sphere.

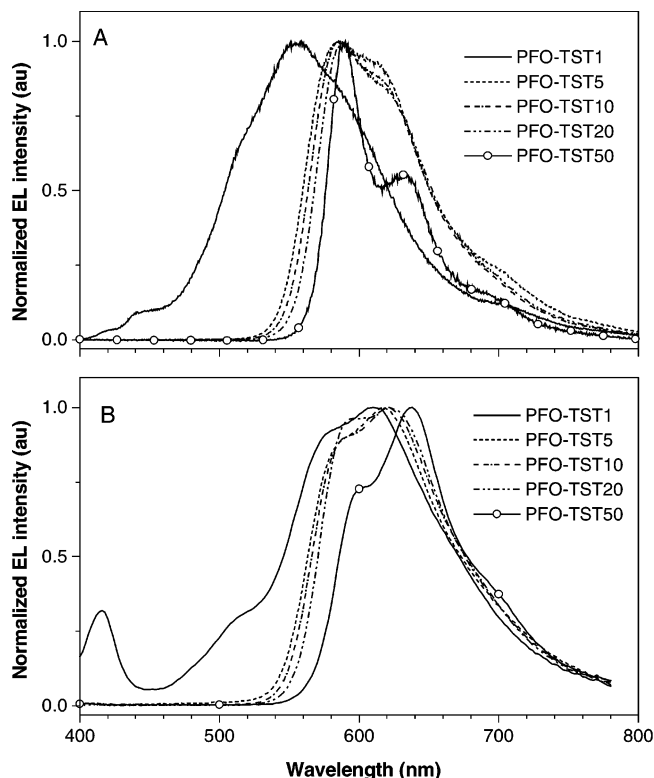


Figure 5. EL spectra of the copolymers with device configurations of (A) ITO/PEDOT/copolymer/Ba/Al and (B) ITO/PEDOT/PVK/copolymer/Ba/Al.

role of the intramolecular energy transfer in the PL emission.

Photoluminescence spectra of the thin solid films of the copolymers are shown in Figure 4B. The PL peaks and the absolute PL quantum yields (QEs) are also listed in Table 3. Once the TST unit is incorporated into the PFO main chain, the PL emission is changed dramatically. Even for PFO-TST1, the blue emission of the PFO segment becomes very weak and the copolymer shows a stronger green emission peak at 510 nm. This can be attributed to strong intermolecular energy transfer or partial excimer formation of PFO segment²⁷ in the aggregation state. The QE of the copolymer is 15.2%. For the other four copolymers, the emission signature of PFO at 458 nm is gradually weakened and disappears finally. The silole emission also continuously red shifts to the red light region. The QE of PFO-TST5 is the highest among the five copolymers.

Electroluminescence Properties. A double-layer device with a configuration of ITO/PEDOT (50 nm)/copolymer (80 nm)/Ba/Al was fabricated. The EL spectra of the copolymers are shown in Figure 5A. For PFO-TST1, the EL spectrum is very broad and peaks at 556 nm, close to white light on the basis of CIE coordinates

Table 4. EL Properties of the Copolymers with a Device Configuration of ITO/PEDOT/Copolymer/Ba/Al^a

copolymer	bias (V)	current (mA)	brightness (cd/m ²)	η^b (%)	λ_{\max} (nm)	CIE <i>x, y</i>
PFO-TST1	7.8	4.4	73	0.21	556	0.30, 0.39
PFO-TST5	11.8	5.3	140	0.39	585	0.58, 0.42
PFO-TST10	8.6	5.2	101	0.28	586	0.59, 0.40
PFO-TST20	7.2	4.8	36	0.11	590	0.61, 0.39
PFO-TST50	3.2	4.9	2	0.01	590, 633	0.62, 0.38

^a The active area is 0.15 cm². ^b External quantum efficiency.

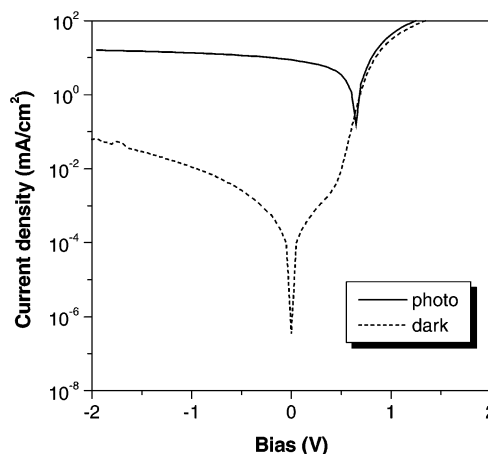
Table 5. EL Properties of the Copolymers with a Device Configuration of ITO/PEDOT (50 nm)/PVK (30 nm)/Copolymer (80 nm)/Ba/Al

copolymer	bias (V)	current (mA)	brightness (cd/m ²)	η^b (%)	λ_{\max} (nm)	CIE <i>x, y</i>
PFO-TST1	14.6	5.5	186	0.89	610	0.49, 0.42
PFO-TST5	17.2	5.3	97	0.48	618	0.59, 0.40
PFO-TST10	16.8	5.1	77	0.40	622	0.60, 0.40
PFO-TST20	13.4	5.6	94	0.44	624	0.61, 0.39
PFO-TST50	12.2	4.7	30	0.17	638	0.63, 0.36

^a The active area is 0.15 cm². ^b External quantum efficiency.

of the EL spectrum (Table 4). This is also a signature of incomplete intra- and intermolecular energy transfer from the PFO segment to the silole moiety due to the low content of TST or partial excimer formation of the PFO segment. The EL spectrum of PFO-TST5 demonstrates that a complete energy transfer is fulfilled at a TST content of 5%. The silole moiety even at the low content can serve as an efficient trap for all of the generated excitons. As a result, the generated excitons are confined and recombined on the silole sites, and the copolymer emits exclusively from the narrow band gap component. Increasing the TST contents to 10% and 20%, their EL spectra are quite similar to that of PFO-TST5. Different from the two comparable peaks at 591 and 616 nm of the PL spectrum of PFO-TST50, its EL spectrum shows a main peak at 590 nm and a shoulder peak at 633 nm. All the EL spectra of the copolymers are red shifted to the corresponding PL spectra of their films. Similar results were reported before.¹² The device performances are also listed in Table 4. At a current of ~5 mA, the EL device with PFO-TST5 as the emissive layer shows the highest external quantum efficiency ($\eta = 0.39\%$). Among the devices, the highest brightness is 1226 cd/m² at 11.0 V, obtained by the white light device with PFO-TST1 as the emissive layer. The turn-on voltage of PFO-TST50 is as low as 2.67 V; however, its η is only 0.01%.

Since the HOMO for the copolymer is around 5.71–5.75 eV (Table 2), while the work function of PEDOT is around 5.0–5.2 eV, it would be possible to expect a better hole injection once a PVK (work function 5.5–5.6 eV) is used as the hole injection anode. So we further fabricated EL devices with a configuration of ITO/PEDOT (50 nm)/PVK (30 nm)/copolymer (80 nm)/Ba/Al. The EL spectra of the devices are shown in Figure 5B. All the peaks of the EL spectra are red shifted compared to those of the EL devices without a PVK layer. For PFO-TST5–50, exchange of the emission peaks and shoulders was found when the PVK layer was inserted. This might be attributed to different contributions of phonon vibration, and also possibly due to a microcavity effect.²⁸ Better red light CIE coordinates were achieved (Table 5). Despite the increasing voltage to reach a current of ~5 mA, the η for every copolymer was increased, indicating that the recombination of an

**Figure 6.** Photocurrent and dark current of the PVC device with PFO-TST50:PCBM = 1:4 as the active layer. The photocurrent was recorded under an AM1.5 solar simulator at 100 mW/cm².**Table 6. Photovoltaic Properties of the Copolymers^a**

active layer	V_{oc}^b (V)	I_{sc}^c (mA/m ²)	FF ^d (%)	ECE ^e (%)
PFO-TST50:PCBM = 1:2	0.70	5.40	31.5	1.20
PFO-TST50:PCBM = 1:4	0.65	8.67	35.8	2.01

^a With a device configuration of ITO/PEDOT/active layer/Ba/Al. ^b Open-circuit voltage. ^c Short-circuit current. ^d Fill factor. ^e Energy conversion efficiency.

injected electron and hole was improved with the insertion of the PVK layer.

Photovoltaic Properties. In the fabrication of bulk-heterojunction photovoltaic cells, methanofullerene [6,6]-phenyl C61-butyric acid methyl ester (PCBM) is the typical electron acceptor.³ On the basis of the UV absorptions of the films of the PFO-TST copolymers, PFO-TST50, the alternating copolymer, possesses the best spectral coverage range of the visible light. The HOMO and LUMO levels of PFO-TST50 also match that of an electron donor for bulk-heterojunction photovoltaic cells with a PCBM acceptor. Thus, PFO-TST50 was chosen to fabricate photovoltaic cells with a configuration of ITO/PEDOT/PFO-TST50:PCBM/Ba/Al. The energy conversion efficiency (ECE) and fill factor (FF) were calculated according to the following equations:³

$$EQE = (FF)J_{sc}V_{oc}/P_{in}$$

$$FF = J_m V_m / J_{sc} V_{oc}$$

where P_{in} is the incident radiation flux, J_{sc} and V_{oc} are the short-circuit current and open-circuit voltage, respectively, and J_m and V_m are the current and voltage at the maximum power output, respectively.

The J - V characteristic of a PVC device with PFO-TST50:PCBM = 1:4 as the active layer is shown in Figure 6 as an example. The dark J - V curve shows a small leakage current, suggesting a continuous, pinhole-free active layer in the device. Energy conversion efficiencies were measured under an AM1.5 solar simulator at 100 mW/cm². The photovoltaic performances of the devices are summarized in Table 6. At a 1:2 ratio of PFO-TST50 to PCBM, the J_{sc} , V_{oc} , and FF are 5.4 mA/m², 0.7 V, and 31.5%, respectively. The ECE was further improved to 2.01% by using PFO-TST50:PCBM = 1:4 as the active layer, which is among the highest values so far reported for bulk-heterojunction photovoltaic

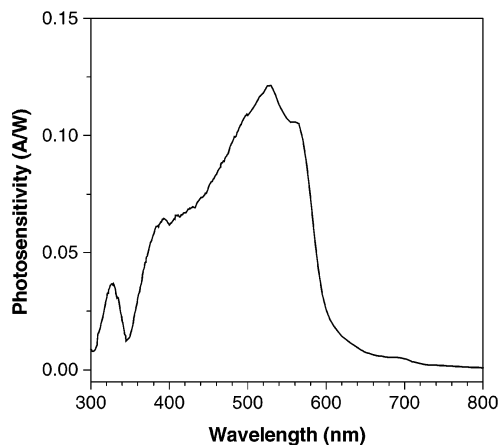


Figure 7. Spectral response of the photovoltaic cell with PFO-TST50:PCBM = 1:4 as the active layer.

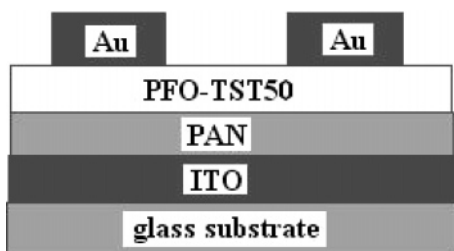


Figure 8. Schematic structure of the FET device.

cells.^{3,13} Donor:PCBM = 1:4 is also the optimal ratio for MEH-PPV and another fluorene-containing alternating copolymer (PFDTBT).¹³ The V_{oc} of the device slightly decreases but with higher FF, compared with those of PFO-TST50:PCBM = 1:2 as the active layer. The V_{oc} values of our devices are relatively lower than those of MEH-PPV and PFDTBT devices, but J_{sc} of the device with PFO-TST50:PCBM = 1:4 is remarkably higher than those of MEH-PPV and PFDTBT devices. The spectral response of the device with PFO-TST50:PCBM = 1:4 was measured (Figure 7). The spectral response peaks at 528 nm with a photosensitivity of 0.12 A/W, all comparable to the corresponding values of MEH-PPV.^{13b} The spectral response of the device is quite similar to the absorption spectrum of the film of PFO-TST50.

Field Effect Hole Mobility. Carrier mobilities play an important role in bulk-heterojunction PVCs. PFO-TST50, the alternating copolymer, should possess enough high hole mobility on the basis of its good electron donor performance in the PVC. To measure the hole mobility of PFO-TST50, we fabricated an FET device with a top contact configuration of ITO (110 nm)/polyacrylonitrile (PAN) (450 nm)/PFO-TST50 (80 nm)/Au (50 nm), as shown in Figure 8. The width to length ratio (W/L) of the FET device is 100. Introduction of a polymeric insulator for the gate electrode is an important step toward fully organic FET. Here PAN was utilized as a novel organic insulator for the ITO gate electrode.²⁹ We made a parallel capacitor, indicating the capacitance (C_i) of the PAN film (450 nm) was 12.4 nF/cm². The dielectric constant (ϵ) was calculated to be 6.27, which is higher than that of cross-linked poly(vinylphenol) (PVP) ($\epsilon = 5$) but lower than that of poly(vinyl alcohol) (PVA) ($\epsilon = 10$).³⁰ The breakdown electric field of the capacitor was ~ 1 MV/cm.

The output and transfer characteristics of the FET device are shown in Figure 9. At different gate voltages

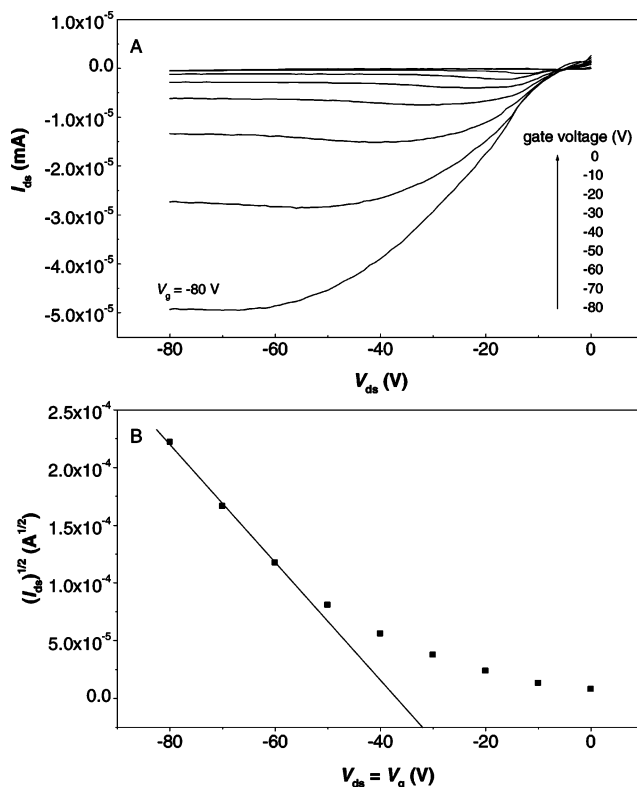


Figure 9. Output and transfer characteristics of the FET device: (A) I_{ds} vs V_{ds} for a series of gate voltages and (B) $(I_{ds})^{1/2}$ vs V_{ds} with gate voltage equivalent to V_{ds} .

(V_g), the drain current (I_{ds}) of the device could reach saturation along with the drain voltage (V_{ds}) (Figure 9A). The on/off current ratio is ~ 100 . To calculate the hole mobility (μ) from the curve of $(I_{ds})^{1/2}$ vs V_{ds} , the gate voltage was set equivalent to the drain voltage to ensure saturated I_{ds} .³¹ The field effect hole mobility was estimated in the saturation regime using the following equation:³²

$$I_{ds} = (W/2L)\mu C_i (V_g - V_{th})^2$$

where V_{th} is the threshold voltage.

From the slope of the line as shown in Figure 9B,³¹ the hole mobility of PFO-TST50 is estimated to be 4.5×10^{-5} cm²/(V s), which is higher than that of MDMO-PPV and Dow Red PF.³³ The V_{th} of the device is -32 V.

An electron-only FET device with aluminum as the source and drain electrodes was also fabricated, but the FET performance was not successful. So PFO-TST50 is probably a p-type semiconducting polymer.

Conclusions

In summary, a novel series of soluble conjugated random and alternating copolymers (PFO-TST) derived from 9,9-dioctylfluorene (FO) and 1,1-dimethyl-3,4-diphenyl-2,5-bis(2'-thienyl)silole (TST) were synthesized by palladium(0)-catalyzed Suzuki coupling reactions. The random copolymers exhibited PFO-segment-dominated UV absorption and narrow band gap TST absorption. For the alternating copolymer, only a broad absorption band was found, demonstrating a mixed and TST-dominated electronic configuration. Compared with the solution PL, complete PL excitation energy transfer from the PFO segment to TST unit could be achieved by film PL at lower TST content. By using the copoly-

mers as active layers, three kinds of organic semiconductor devices, PLEDs, PVCs, and FET, were demonstrated. Red light PLEDs were achieved for the silole-containing polymers. With the alternating copolymer as the electron donor, an energy conversion efficiency of 2.01% was realized under an AM1.5 simulated solar light at 100 mW/cm². The field effect hole mobility of the alternating copolymer is 4.5×10^{-5} cm²/(V s) using polyacrylonitrile as an organic dielectric layer.

Acknowledgment. Financial support from the Natural Science Foundation of China (Grants 50303006 and 50373014) and Ministry of Science and Technology of China (Grant 2002CB613404) is gratefully acknowledged.

References and Notes

- (1) (a) Burroughes, J. H.; Bradley, D. D. C.; Brown, A. R.; Marks, R. N.; Mackay, K.; Friend, R. H.; Burns, P. L.; Holmes, A. B. *Nature (London)* **1990**, *347*, 539. (b) Braun, D.; Heeger, A. J. *Appl. Phys. Lett.* **1991**, *58*, 982. (c) Burns, P. L.; Holmes, A. B.; Kraft, A.; Bradley, D. D. C.; Brown, A. R.; Friend, R. H.; Gymer, R. W. *Nature (London)* **1992**, *356*, 47. (d) Gustafsson, G.; Cao, Y.; Treacy, G. M.; Klavetter, F.; Colaneri, N.; Heeger, A. J. *Nature (London)* **1992**, *357*, 477. (e) Pei, Q.; Yu, G.; Zhang, C.; Yang, Y.; Heeger, A. J. *Science* **1995**, *269*, 1086.
- (2) For reviews, see the following. (a) Sugura, J. L. *Acta Polym.* **1998**, *49*, 319. (b) Kraft, A.; Grimsdale, A. C.; Holmes, A. B. *Angew. Chem., Int. Ed.* **1998**, *37*, 402. (c) Kim, D. Y.; Cho, H. N.; Kim, C. Y. *Prog. Polym. Sci.* **2000**, *25*, 1089. (d) Bernius, M.; Inbasekaran, M.; O'Brien, J.; Wu, W. *Adv. Mater.* **2000**, *12*, 1737. (e) Akcelrud, L. *Prog. Polym. Sci.* **2003**, *28*, 875.
- (3) (a) Sariciftci, N. S.; Smilowitz, L.; Heeger, A. J.; Wudl, F. *Science* **1992**, *258*, 1474. (b) Yu, G.; Gao, J.; Hummelen, J. C.; Wudl, F.; Heeger, A. J. *Science* **1995**, *270*, 1789. (c) Brabec, C. J.; Padinger, F.; Sariciftci, N. S.; Hummelen, J. C. *J. Appl. Phys.* **1999**, *85*, 6866. (d) Coakley, K. M.; McGehee, M. *Chem. Mater.* **2004**, *16*, 4533.
- (4) (a) Bao, Z.; Dodabalapur, A.; Lovinger, A. J. *Appl. Phys. Lett.* **1996**, *69*, 4108. (b) Garnier, F.; Horowitz, G.; Fichou, D.; Yassar, A. *Synth. Met.* **1996**, *81*, 163.
- (5) (a) Heibner, T. R.; Wu, C. C.; Marcy, D.; Lu, M. H.; Sturm, J. C. *Appl. Phys. Lett.* **1998**, *72*, 519. (b) Chang, S. C.; Liu, J.; Bharathan, J.; Yang, Y.; Onohara, J.; Kido, J. *Adv. Mater.* **1998**, *11*, 734.
- (6) (a) Hoppe, H.; Sariciftci, N. S. *J. Mater. Res.* **2004**, *19*, 1924. (b) Brabec, C. J.; Sariciftci, N. S.; Hummelen, J. C. *Adv. Funct. Mater.* **2001**, *11*, 15.
- (7) (a) Zhan, X.; Liu, Y.; Wu, X.; Wang, S.; Zhu, D. *Macromolecules* **2002**, *35*, 2529. (b) Ding, J.; Day, M.; Robertson, G.; Roovers, J. *Macromolecules* **2002**, *35*, 3474. (c) Wu, F. I.; Reddy, D. S.; Shu, C. F.; Liu, M. S.; Jen, A. K. Y. *Chem. Mater.* **2003**, *15*, 269. (d) Li, Y.; Ding, J.; Day, M.; Tao, Y.; Lu, J.; Diorio, M. *Chem. Mater.* **2004**, *16*, 2165. (e) Fang, Q.; Yamamoto, T. *Macromolecules* **2004**, *37*, 5894.
- (8) (a) Huang, F.; Wu, H.; Wang, D.; Yang, W.; Cao, Y. *Chem. Mater.* **2004**, *16*, 708. (b) Huang, F.; Hou, L.; Wu, H.; Wang, X.; Shen, H.; Cao, W.; Yang, W.; Cao, Y. *J. Am. Chem. Soc.* **2004**, *126*, 9845. (c) Wu, H.; Huang, F.; Mo, Y.; Yang, W.; Wang, D.; Peng, J.; Cao, Y. *Adv. Mater.* **2004**, *16*, 1826.
- (9) (a) Pei, Q.; Yang, Y. *J. Am. Chem. Soc.* **1996**, *118*, 7146. (b) Ranger, M.; Rondeau, D.; Leclerc, M. *Macromolecules* **1997**, *30*, 7686.
- (10) (a) Bernius, M.; Inbasekaran, M.; Woo, E.; Wu, W.; Wujkowsky, L. *J. Mater. Sci.: Mater. Electron.* **2000**, *11*, 111. (b) Lim, E.; Jung, B. J.; Shim, H. K. *Macromolecules* **2003**, *36*, 4288. (c) Cho, N. S.; Hwang, D. H.; Jung, B. J.; Lim, E.; Lee, J.; Shim, H. K. *Macromolecules* **2004**, *37*, 5265.
- (11) (a) Herguth, P.; Jiang, X.; Liu, M. S.; Jen, A. K. Y. *Macromolecules* **2002**, *35*, 6094. (b) Liu, M. S.; Jiang, X.; Liu, S.; Herguth, P.; Jen, A. K. Y. *Macromolecules* **2002**, *35*, 3522.
- (12) (a) Hou, Q.; Xu, Y.; Yang, W.; Yuan, M.; Peng, J.; Cao, Y. *J. Mater. Chem.* **2002**, *12*, 2887. (b) Niu, Y. H.; Hou, Q.; Cao, Y. *Appl. Phys. Lett.* **2003**, *82*, 2163. (c) Yang, R.; Tian, R.; Yang, Y.; Hou, Q.; Cao, Y. *Macromolecules* **2003**, *36*, 7453. (d) Yang, J.; Jiang, C.; Zhang, Y.; Yang, R.; Yang, W.; Hou, Q.; Cao, Y. *Macromolecules* **2004**, *37*, 1211. (e) Hou, Q.; Zhou, Q.; Zhang, Y.; Yang, W.; Yang, R.; Cao, Y. *Macromolecules* **2004**, *37*, 6299.
- (13) (a) Svensson, M.; Zhang, F.; Veenstra, S. C.; Verhees, W. J. H.; Hummelen, J. C.; Kroon, J. M.; Inganas, O.; Andersson, M. R. *Adv. Mater.* **2003**, *15*, 988. (b) Zhou, Q.; Hou, Q.; Zheng, L.; Deng, X.; Yu, G.; Cao, Y. *Appl. Phys. Lett.* **2004**, *84*, 1653.
- (14) (a) Yamaguchi, S.; Tamao, K. *J. Chem. Soc., Dalton Trans.* **1998**, 3693. (b) Hissler, M.; Dyer, P. W.; Reau, R. *Coord. Chem. Rev.* **2003**, *244*, 1.
- (15) (a) Murata, H.; Malliaras, G. G.; Uchida, M.; Shen, Y.; Kafafi, Z. H. *Chem. Phys. Lett.* **2001**, *339*, 161. (b) Tamao, K.; Uchida, M.; Izumizawa, T.; Furukawa, K.; Yamaguchi, S. *J. Am. Chem. Soc.* **1996**, *118*, 11974.
- (16) (a) Chen, J.; Law, C. C. W.; Lam, J. W. Y.; Dong, Y.; Lo, S. M. F.; Williams, I. D.; Zhu, D.; Tang, B. Z. *Chem. Mater.* **2003**, *15*, 1535. (b) Luo, J.; Xie, Z.; Lam, J. W. Y.; Cheng, L.; Chen, H.; Qiu, C.; Kwok, H. S.; Zhan, X.; Liu, Y.; Zhu, D.; Tang, B. Z. *Chem. Commun.* **2001**, 1740.
- (17) Murata, H.; Kafafi, Z. H.; Uchida, M. *Appl. Phys. Lett.* **2002**, *80*, 189.
- (18) (a) Chen, H.; Chen, J.; Qiu, C.; Tang, B. Z.; Wong, H.; Kwok, H. S. *IEEE J. Sel. Top. Quantum Electron.* **2004**, *10*, 10. (b) Chen, H. Y.; Lam, J. W. Y.; Luo, J. D.; Ho, Y. L.; Tang, B. Z.; Zhu, D. B.; Wong, M.; Kwok, H. S. *Appl. Phys. Lett.* **2002**, *81*, 574.
- (19) Liu, M. S.; Luo, J.; Jen, A. K. Y. *Chem. Mater.* **2003**, *15*, 3496.
- (20) (a) Chen, J.; Xie, Z.; Lam, J. W. Y.; Law, C. C. W.; Tang, B. Z. *Macromolecules* **2003**, *36*, 1108. (b) Chen, J.; Peng, H.; Law, C. C. W.; Dong, Y.; Lam, J. W. Y.; Williams, I. D.; Tang, B. Z. *Macromolecules* **2003**, *36*, 4319.
- (21) (a) Yamaguchi, S.; Goto, T.; Tamao, K. *Angew. Chem., Int. Ed.* **2000**, *39*, 1695. (b) Lee, Y.; Sadki, S.; Tsui, B.; Reynolds, J. R. *Chem. Mater.* **2001**, *13*, 2234. (c) Zhang, G.; Ma, J.; Jiang, Y. *Macromolecules* **2003**, *36*, 2130.
- (22) Yamaguchi, S.; Endo, T.; Uchida, M.; Izumizawa, T.; Furukawa, K.; Tamao, K. *Chem.—Eur. J.* **2000**, *6*, 1683.
- (23) With the diboronic ester of TST, it is possible to obtain soluble PFO-TST copolymers with a TST content higher than 50% by the Suzuki coupling reaction.
- (24) Ferman, J.; Kakareka, J. P.; Klooster, W. T.; Mullin, J. L.; Quattrucci, J.; Ricci, J. S.; Tracy, H. J.; Vining, W. J.; Wallace, S. *Inorg. Chem.* **1999**, *38*, 2464.
- (25) Janietz, S.; Bradley, D. D. C.; Grell, M.; Giebeler, C.; Inbasekaran, M.; Woo, E. P. *Appl. Phys. Lett.* **1998**, *73*, 2453.
- (26) Agrawal, A. K.; Jenekhe, S. A. *Chem. Mater.* **1996**, *8*, 579.
- (27) Zeng, G.; Yu, W. L.; Chua, S. J.; Huang, W. *Macromolecules* **2002**, *35*, 6907.
- (28) Bulovic, V.; Khalifin, V. B.; Gu, G.; Burrows, P. E.; Garbuzov, D. Z.; Forrest, S. R. *Phys. Rev. B* **1998**, *58*, 3730.
- (29) Veres, J.; Ogier, S.; Lloyd, G. *Chem. Mater.* **2004**, *16*, 4543.
- (30) Parashkov, R.; Becker, E.; Ginev, G.; Riedl, T.; Johannes, H. H.; Kowalsky, W. *J. Appl. Phys.* **2004**, *95*, 1594.
- (31) Horowitz, G.; Hajlaoui, R.; Bouchriha, H.; Bourguiga, R.; Hajlaoui, M. *Adv. Mater.* **1998**, *10*, 923.
- (32) Sze, S. M. *Physics of Semiconductor Devices*, 2nd ed.; John Wiley & Sons: New York, 1981.
- (33) (a) Choulis, S. A.; Nelson, J.; Kim, Y.; Poplavskyy, D.; Kreouzis, T.; Durrant, J. R.; Bradley, D. D. C. *Appl. Phys. Lett.* **2003**, *83*, 3812. (b) Pacios, R.; Nelson, J.; Bradley, D. D. C.; Brabec, C. J. *Appl. Phys. Lett.* **2003**, *83*, 4764.

MA047561L